Journal of Biogeography (J. Biogeogr.) (2014) 41, 476–488

ORIGINAL ARTICLE

The legacy of mid-Holocene fire on a Tasmanian montane landscape

Michael-Shawn Fletcher[1,2,3]*, Brent B. Wolfe[4], Cathy Whitlock[5], David P. Pompeani[6], Hendrik Heijnis[7], Simon G. Haberle[2], Patricia S. Gadd[7] and David M. J. S. Bowman[8]

[1]Department of Resource Management and Geography, University of Melbourne, Parkville, VIC 3010, Australia, [2]Archaeology and Natural History, College of Asia and the Pacific, The Australian National University, Canberra, ACT 0200, Australia, [3]Institute of Ecology and Biodiversity, University of Chile, Santiago, Chile, [4]Department of Geography and Environmental Studies, Wilfrid Laurier University, Waterloo, ON N2L 3C5, Canada, [5]Institute on Ecosystems, Montana State University, Bozeman, MT 59715, USA, [6]Department of Geology and Planetary Science, University of Pittsburgh, Pittsburgh, PA 15260-3332, USA, [7]Institute for Environmental Research, Australian Nuclear Science and Technology Organisation, Kirrawee, DC NSW 2232, Australia, [8]School of Plant Science, University of Tasmania, Hobart, TAS 7001, Australia

*Correspondence: Michael-Shawn Fletcher, Department of Resource Management and Geography, University of Melbourne, Parkville, VIC 3010, Australia.
E-mail: msfl@unimelb.edu.au

ABSTRACT

Aim To assess the long-term impacts of landscape fire on a mosaic of pyrophobic and pyrogenic woody montane vegetation.

Location South-west Tasmania, Australia.

Methods We undertook a high-resolution multiproxy palaeoecological analysis of sediments deposited in Lake Osborne (Hartz Mountains National Park, southern Tasmania), employing analyses of pollen, macroscopic and microscopic charcoal, organic and inorganic geochemistry and magnetic susceptibility.

Results Sequential fires within the study catchment over the past 6500 years have resulted in the reduction of pyrophobic rain forest taxa and the establishment of pyrogenic *Eucalyptus*-dominated vegetation. The vegetation change was accompanied by soil erosion and nutrient losses. The rate of post-fire recovery of widespread rain forest taxa (*Nothofagus cunninghamii* and *Eucryphia* spp.) conforms to ecological models, as does the local extinction of fire-sensitive rain forest taxa (*Nothofagus gunnii* and Cupressaceae) following successive fires.

Main conclusions The sedimentary analyses indicate that recurrent fires over several centuries caused a catchment-wide transition from pyrophobic rain forest to pyrophytic eucalypt-dominated vegetation. The fires within the lake catchment during the 6500-year long record appear to coincide with high-frequency El Niño events in the equatorial Pacific Ocean, signalling a potential threat to these highly endemic rain forests if El Niño intensity amplifies as predicted under future climate scenarios.

Keywords
***Athrotaxis*, carbon, charcoal particles, *Eucalyptus*, fire, ITRAX, nitrogen, *Nothofagus*, rain forest, Southern Hemisphere.**

INTRODUCTION

Fire is a key ecological agent that has been implicated in the determination of vegetation patterns at scales ranging from local to global (Bond *et al.*, 2005; Bowman *et al.*, 2009). This is no better exemplified than by the ecology of forests dominated by *Eucalyptus* species (Bowman, 2000). Based on molecular dating, it has been proposed that the remarkable ability of *Eucalyptus* to resprout from stems following fire developed more than 60 million years ago (Crisp *et al.*, 2011), and the massive radiation of the > 700 *Eucalyptus* species across Australia is widely understood as an evolutionary response to aridity and fire (Hill, 2004). Temperate *Eucalyptus* forests regenerate via post-fire seedling recruitment and/or resprouting after intense fires and, in the absence of fire, are replaced by continuously regenerating trees that form pyrophobic rain forest (Bowman, 2000). Paradoxically, temperate *Eucalyptus* forests are often juxtaposed against pyrophobic rain forest in south-east Australia and Tasmania. Tasmania hosts the largest remaining vestiges in Australia of the cool temperate rain forest that was widespread across the Australian landscape through much of the Cenozoic, a flora that has close taxonomic links to other Southern Hemisphere forests and fossil assemblages. Of particular note are a number of conifers (e.g. *Athrotaxis* in Cupressaceae and *Lagarostrobos* in Podocarpaceae) that are endemic to the mountains

http://wileyonlinelibrary.com/journal/jbi
doi:10.1111/jbi.12229

Journal of Biogeography

of western Tasmania and that were once more widespread on the Australian mainland (Hill & Carpenter, 1990; Hill, 2004). Accordingly, Tasmania represents the last major interface between pyrophytic *Eucalyptus* forests and a pyrophobic rain forest flora that was once widespread in Australia and which is now confined on the mainland to depauperate rain forest pockets in tiny fire refugia (Bowman, 2000; Hill, 2004; Kershaw *et al.*, 2007). Indeed, the latest loss from the mainland cool temperate rain forest flora was the fire-sensitive conifer *Phyllocladus aspleniifolius* (Labill.) Hook.f. (Podocarpaceae) during the late Quaternary (Head, 1985; McKenzie & Kershaw, 2000), a species now restricted to Tasmania. Thus, the Tasmanian system provides very important insights into the evolutionary and ecological processes that have led to the dominance of pyrophytic *Eucalyptus* communities in Australia. Understanding the dynamics between *Eucalyptus* forests and rain forest is important, because rising temperatures, heightened fire activity and the introduction of *Eucalyptus* plantations over the past century conspire to create conditions that are hostile to the survival of rain forest in Australia and elsewhere in the Southern Hemisphere.

To understand the interaction between fire-sensitive conifers and eucalypts, we undertook a high-resolution multiproxy palaeoecological analysis of sediments deposited in Lake Osborne (Hartz Mountains National Park, southern Tasmania), a site that supports both *Eucalyptus* and the pyrophobic endemic conifer *Athrotaxis selaginoides* D. Don (Cupressaceae). The latter species has suffered landscape-scale losses from postcolonial wildfires, being highly susceptible to all but the lowest intensity surface fires and having limited seed dispersal and slow regeneration which, collectively, have effectively precluded re-establishment in areas burned in the past 40 years (Kirkpatrick & Dickinson, 1984). We hypothesize there are two dominant mechanisms that explain the loss of *Athrotaxis* from Tasmanian landscapes since European settlement commenced in 1802: first, relatively short fire-free intervals (< 100 years) in high-rainfall regions favour eucalypts (Wood *et al.*, 2010); and second, this transition is reinforced because the mobilization and loss of nutrients reduces the growth rates of rain forest trees (mesophytic tree species excluding *Eucalyptus*), reducing canopy closure and hence increasing the fire risk (Jackson, 1968). These fire–vegetation–soil feedbacks are at the heart of a model for western Tasmanian lowland vegetation dynamics known as the 'ecological drift' model (Jackson, 1968; Bowman & Jackson, 1981; Bowman *et al.*, 1986; Wood & Bowman, 2012). Critically, despite the widespread acceptance of this theoretical framework, it remains untested by empirical time-series data and has not been applied to *Athrotaxis* montane forests.

MATERIALS AND METHODS

Geography, climate and vegetation

Tasmania (41–44° S) is a cool temperate continental island that is bisected by a north-west–south-east trending mountain range which intercepts mid-latitude westerly winds, resulting in a steep west-to-east orographic precipitation gradient. The temperature regime is cool (5–7 °C June to August; 14–16 °C December to February), and precipitation exceeds evaporation for most of the year (Sturman & Tapper, 2006). The topography is rugged and complex, with a geological basement composed of low-nutrient-yielding quartz-dominated metasediments and occasional outcrops of rock types with higher nutrient potential, such as dolerite and limestone (Jackson, 1999). The cool, wet climate and often extreme oligotrophy results in an arrested rate of vegetation development in south-west Tasmania, while a long history of human occupation (> 35,000 years) and fire have imparted a significant imprint on the vegetation landscape (Cosgrove, 1999; Bowman & Wood, 2009; Fletcher & Thomas, 2010a; Thomas *et al.*, 2010). Treeless pyrophytic vegetation dominates the landscape (including species of *Melaleuca*, *Leptospermum* and Restionaceae and *Gymnoschoenus sphaerocephalus*) and arboreal communities are restricted by topography and aspect and the protection they afford from fire (Wood *et al.*, 2011). Montane rain forest forms at higher elevations up to the timberline and usually includes *Athrotaxis cupressoides* D. Don, *Athrotaxis selaginoides*, *Nothofagus cunninghamii* (Hook.) Oerst. and *Nothofagus gunnii* (Hook.f.) Oerst. Lower-altitude (lowland) rain forest species include *N. cunninghamii*, *Phyllocladus aspleniifolius*, *Eucryphia lucida* (Labill.) Baill., *Atherosperma moschatum* Labill. and *Anodopetalum biglandulosum* (A. Cunn. ex Hook.) Hook.f. (Harris & Kitchener, 2005). Eucalypt forest forms in areas of moderate fire frequency (*c.* 70–400 year fire return intervals) and occurs as emergent *Eucalyptus* species over a rain forest canopy (Jackson, 1968). Common shrubland and moorland taxa include species of *Melaleuca*, *Leptospermum* and Restionaceae and *Gymnoschoenus sphaerocephalus* (moorland dominant) (Harris & Kitchener, 2005).

Study site: Lake Osborne

Lake Osborne (43°12′53″ S, 146°45′30″ E) is a small moraine-bound subalpine (924 m a.s.l.) lake located on the eastern flank of the Hartz Range in southern Tasmania, Australia (Fig. 1) – an area that lies at the margins of the superhumid western zone of Tasmania. Average annual rainfall at the Keogh's Pimple climate station in the Hartz Range (43°12′0″ S, 146°46′12″ E; 831 m a.s.l.; 1.8 km north of Lake Osborne) is 981.7 mm yr^{-1} (mostly in spring; Fig. 1). The small catchment (0.21 km^2) is characterized by a gentle gradient (0.37) over the 400 m from the lake shore to the highest point in the catchment (1075 m a.s.l.). The vegetation of the catchment is low and shrubby, displaying the clear effects of fire, and substantial areas of bedrock (dolerite) are exposed within the catchment.

Dominant species locally include *Eucalyptus coccifera* Hook.f., *Nothofagus cunninghamii*, *Eucryphia milliganii* Hook.f., *Gahnia grandis* and a number of proteaceous species (including *Bellendena montana*, *Orites revolutus*, *Hakea*

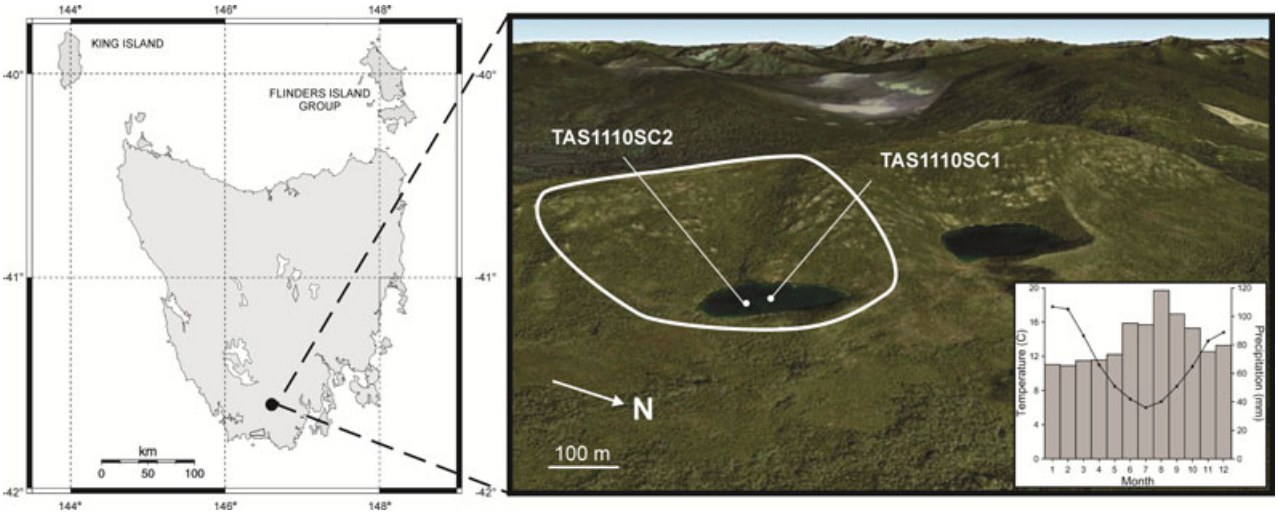

Figure 1 Map showing the location of Lake Osborne in Tasmania and an oblique image of the study area sourced from Google Earth. Inset: a climate graph showing mean monthly temperature (line) and mean monthly rainfall (bars) at Keogh's Pimple (1.8 km north of Lake Osborne) (Australian Bureau of Meteorology, Melbourne, Australia).

lissosperma and *Telopea truncata*). A few fire-scarred individuals of *Athrotaxis selaginoides* grow around the lake's shore but are absent from the rest of the catchment. The local geology is composed of Jurassic dolerite, which, although oligotrophic on a global scale, has a relatively high nutrient yield when compared with the Precambrian and Ordovician quartz-dominated metasediments that outcrop across much of the south-west of the island.

Core collection and magnetic susceptibility

Two cores were retrieved from the deepest (10 m) part of the Lake Osborne basin using a 6-cm-diameter polycarbonate chamber attached to a universal gravity corer. The entire cores were packaged in the field and transported to the laboratory for analyses where they were logged with a Bartington magnetic susceptibility scanner at 1-cm intervals (Bartington Instruments, Witney, UK) and split with a Geotek core splitter (Geotek, Daventry, UK).

Chronology

The chronology of the sediment cores is based on a combination of five ^{210}Pb and ^{137}Cs analyses (using the constant rate of supply model) (Appleby & Oldfield, 1978; Binford, 1990) with the AD 1963/64 global ^{137}Cs peak as a chronostratigraphic marker. Radioisotope (^{210}Pb, ^{137}Cs and ^{214}Pb) activities were determined by direct gamma counting after a three-week equilibration period using a high-purity, broad-energy germanium detector (Canberra BE-3825) at the University of Pittsburgh, Pittsburgh, PA, USA. Nine radiocarbon samples were analysed at the NoSAMS radiocarbon laboratory in Woods Hole, MA, USA. Radiocarbon years were calibrated using the Southern Hemisphere calibration curve (McCormac *et al.*, 2004) to calendar years before present (cal. yr BP; AD 1950). Age–depth modelling of the composite chronology was performed using the CLAM package for R, which allows the interrogation of range age–depth models (R Core Development Team, 2008; Blaauw, 2010).

Palynology

Pollen, spore and microscopic charcoal analyses followed standard protocols (Faegri & Iversen, 1989). Relative pollen data were calculated from a basic pollen sum that included at least 300 pollen grains of terrestrial origin per sample (excluding terrestrial pteridophyte taxa). The percentages of aquatic and pteridophyte taxa are based on a supersum that includes the basic pollen sum, the sum of aquatic taxa and the sum of pteridophyte spores. Fossil pollen zones were identified with the aid of CONISS (Grimm, 1987) and are based on a square-root transformation of the relative (percentage) terrestrial fossil pollen data only. Accumulation rate (per unit time) data were calculated for pollen, algal cysts (*Botryococcus* spp.) and microscopic charcoal fragments by dividing concentration values (calculated by adding a *Lycopodium* spp. spike) by deposition time (yr cm^{-1}).

Macroscopic charcoal analysis

Macroscopic charcoal content of 5-mm thick contiguous sediment samples (1–1.5 cm^3) were analysed to document the local fire history. The sediment samples were digested in 40% hydrogen peroxide and sieved using 125-μm and 250-μm mesh diameters (Whitlock & Larsen, 2001). Time-series analysis of the charcoal data was performed using CharAnalysis (Higuera *et al.*, 2009) by interpolating charcoal counts to the median sample resolution (34 cal. yr) to produce equally spaced intervals and calculating charcoal accumulation rates (CHAR, particles cm^{-2} yr^{-1}). Charcoal peaks, a statistically

robust proxy for local fire episodes (Higuera *et al.*, 2010), were identified as the positive residuals exceeding the 95th percentile threshold of a locally fitted Gaussian mixture CHAR background model (smoothed to 500 years).

Elemental organic carbon and nitrogen analysis

Analysis of organic carbon (C) and nitrogen (N) content of the lake sediments was conducted at 5-mm intervals using an elemental analyser on samples that were pretreated with 10% (by volume) HCl at 60 °C to remove carbonate minerals and shells, followed by freeze-drying and sieving (500 μm) to remove coarse organic debris that may be of terrestrial origin. C and N values are expressed as percentage weight values and the carbon:nitrogen ratio (C:N) is expressed as a weight ratio.

ITRAX analysis

The ITRAX X-ray fluorescence core scanner at the Australian Nuclear Science and Technology Organisation (ANSTO) provided 1-mm interval, non-destructive elemental analyses of the surface of the split cores. Density and colour formation were provided through X-radiography and digital RGB optical images. A calcium:titanium (Ca:Ti) ratio was calculated to estimate the non-detrital calcium content of the lake sediments.

Statistical analyses

Detrended correspondence analysis (DCA) (Hill & Gauch, 1980) was performed on the relative (percentage) terrestrial pollen values using DECORANA in PC-ORD 4.25 (McCune & Mefford, 1999). Cross-correlation analysis was performed on the pollen accumulation rates (PAR), macroscopic charcoal accumulation rates (CHAR) and C and N composition of the lake sediments (cf. Green, 1981). Cross-correlation measures the dependence of values in one time-series on past or future values in another time-series (Green, 1981). PSIMPOLL (Bennett, 2005) was employed to interpolate all data to the median age interval between samples (65 yr) prior to cross-correlation analysis using the statistical software package SPSS v.16 (SPSS, Chicago, IL, USA).

RESULTS

Core collection and magnetic susceptibility

Two cores were retrieved from the deepest part of Lake Osborne: TAS1110SC1 (85 cm) and TAS1110SC2 (91 cm). Both cores consisted of broadly homogeneous organic lake mud that was orange/brown in colour, darkening to brown toward the base of the core (see Appendix S1 in Supporting Information). The magnetic susceptibility analysis revealed virtually identical magnetic profiles for TAS1110SC1 and TAS1110SC2 (Appendix S1). Core TAS1110SC2 was selected for destructive analyses, while TAS1110SC1 was reserved for non-destructive scanning XRF analysis.

Chronology

Radiometric analyses were performed on TAS1110SC2 (Tables 1 & 2, Fig. 2). A maximum radiocarbon age of 6089 ± 80 cal. yr BP was obtained at a depth of 85 cm, while the AD 1964 bomb peak in ^{137}Cs was located between 0.5 and 1.5 cm depth. The age–depth model (Fig. 2) is based on a locally smoothed (0.4) spline regression and is remarkably linear. Sediment accumulation rates were slow, with a median rate of 67.4 yr cm^{-1}.

Palynology

A total of 107 samples were analysed for pollen, spore and microscopic charcoal analyses. Two main pollen zones (Zone 1, 91–35 cm; Zone 2, 34.5–0 cm) and a series of subzones were identified with the aid of CONISS (Fig. 3, Table 3). Pollen accumulation rates (PAR) for selected taxa are presented in Fig. 4, along with microscopic CHAR. Arboreal taxa (Cupressaceae, *N. cunninghamii*, *Eucryphia*, *P. aspleniifolius* and *Eucalyptus*) made up 60–90% of the terrestrial PAR throughout the sequence and each pollen type displayed clear trends associated with changes in microscopic (and macroscopic) CHAR (Fig. 4).

The pollen record was divided into two zones: rain forest (Zone 1) and *Eucalyptus* forest (Zone 2). Zone 1 is divided into three subzones based on CONISS. Subzone 1a (6452–5786 cal. yr BP) is dominated by *Nothofagus gunnii* (13–19%), Cupressaceae (12–18%) and *N. cunninghamii* (26–30%). Subzone 1b (5786–3525 cal. yr BP) is dominated by *N. cunninghamii* (29–43%) and Cupressaceae (5–10%), with the latter displaying a distinct increase and subsequent decrease towards the top of the zone in an inverse relationship with *Eucryphia* (3–8%). Subzone 1c is dominated by Cupressaceae (3–20%) and *N. cunninghamii* (31–44%).

Zone 2 is divided into two subzones based on CONISS. Subzone 2a is dominated by *N. cunninghamii* (26–41%) and *Eucalyptus* (11–20%), with a sharp increase in *Eucryphia* (2–9%) towards the top of the zone. Subzone 2b is dominated by *Eucalyptus* (14–36%) and *N. cunninghamii* (14–31%), with a notable increase in Proteaceae (1–4%).

Macroscopic charcoal

Macroscopic CHAR values were generally low throughout the record, with statistically significant peaks at *c.* 5856, 5244, 5006, 4032, 2966, 2626, 348 and −26 calendar years (AD 1976) before present (cal. yr BP) (Fig. 4, Appendix S2).

Elemental organic carbon and nitrogen analysis

The most striking stratigraphic change in the C and N elemental data occurred immediately after macroscopic CHAR

Table 1 Table showing the results of the ^{210}Pb and ^{137}Cs analyses of sediment core TAS1110SC2 from Lake Osborne, southern Tasmania. The calculated ages are based on the constant rate of supply model (CRS), employing the ^{137}Cs peak as a chronostratigraphic marker (AD 1964/63), and the coring year (2010) at a depth of 0 cm. '< det' indicates levels below detection limits.

Depth (cm)	^{210}Pb (Bq g^{-1})	^{214}Pb (Bq g^{-1})	Cumulative weight influx (g cm^{-2})	CRS age (cal. yr BP)	Error (years)	^{137}Cs (Bq g^{-1})	1s error
0.5	0.3100	0.0519	0.090	−19	11.41	< det	0
1.5	0.1330	0.0619	0.173	17	21.85	0.018	0.0095
2.5	0.0757	0.0459	0.268	n/a	n/a	< det	n/a
3.5	< det	0.0390	0.371	n/a	n/a	< det	n/a
4.75	< det	0.0820	0.512	n/a	n/a	< det	n/a

Table 2 Table showing the results of the radiocarbon dating of sediment core TAS1110SC2 from Lake Osborne, southern Tasmania. Upper and lower ranges are based on 2-sigma error ranges. Calibrations are based on the Southern Hemisphere calibration curve of McCormac *et al.* (2004).

			Calibrated ages (cal. yr BP)		
Depth (cm)	Radiocarbon age (^{14}C yr BP)	Error (^{14}C yr BP)	Median	Lower range	Upper range
8	985	25	838	764	893
15	1440	30	1305	1278	1344
21	1720	25	1576	1530	1662
25	1940	25	1827	1753	1882
39	2960	25	3043	2939	3162
50	3500	25	3715	3632	3821
65	4260	25	4736	4623	4836
85	5360	40	6089	5954	6245

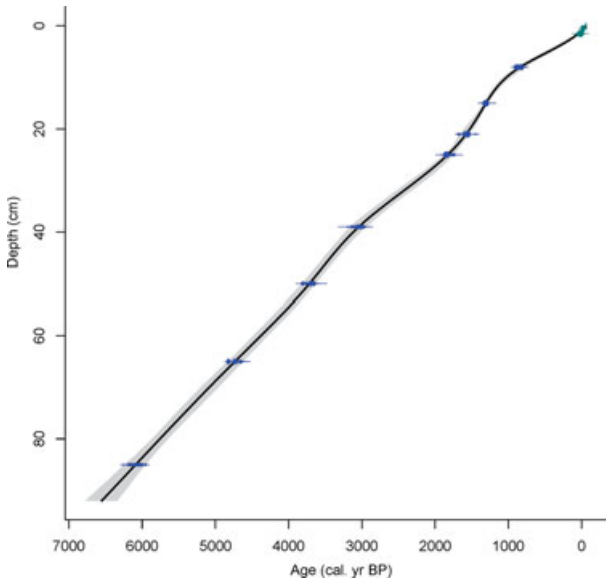

Figure 2 The age–depth model for TAS1110SC2 based on a smooth spline (smoothing factor 0.4) regression and constructed using clam (Blaauw, 2010).

peaks (Fig. 5), with negative trends in both C and N content of the sediments and initially high then decreasing C:N values. Every statistically significant macroscopic CHAR peak prior to *c.* 2600 cal. yr BP coincided with a decrease in C and N elemental values, reflecting a high biogeochemical sensitivity of the lake sediments to fire episodes within the local catchment. The period after *c.* 2600 cal. yr BP was marked by lower-amplitude variations in C and N content and by relatively constant and low C:N ratio values through to the present. C:N values throughout the entire record were consistently higher than expected for aquatic organic matter and are more indicative of terrestrial organic matter in non-nitrogen-limited systems (Meyers & Teranes, 2001).

ITRAX analysis

Selected elemental data obtained by the ITRAX analysis revealed increases in iron (Fe) in association with increases in magnetic susceptibility following the statistically significant CHAR peaks at *c.* 5856, 4632 and 2966 cal. yr BP (Fig. 6). Titanium (Ti) largely tracked Fe throughout the profile. Dysprosium, a rare earth element contained in Tasmanian Jurassic dolerite (Duncan, 2003), registered low values consistent with its rarity, with a persistent increase after *c.* 3800 cal. yr BP. Calcium (Ca) was corrected for detrital Ca using Ti as a detrital divisor (Ca:Ti). Non-detrital Ca was initially high prior to the first macroscopic CHAR peak in the record (*c.* 5856 cal. yr BP), after which values decreased sharply. Indeed, sharp decreases in non-detrital Ca occurred after each of the macroscopic CHAR peaks mentioned above (*c.* 5856, 4632 and 2966 cal. yr BP), whereas increases in non-detrital Ca occurred between these CHAR peaks in tandem with Cupressaceae PAR.

Statistical analyses

The DCA biplot presented in Fig. 7 shows correlations between pollen taxa and the ordination axes. DCA axis 1 explains 77.8% of the variance in the pollen dataset and is significantly correlated with abundance of key arboreal taxa [Cupressaceae, *N. gunnii* (positive) and *Eucalyptus* (negative)]. DCA axis 2 explains only 3.3% of variance in the dataset and is weakly correlated with *P. aspleniifolius* and Cupressaceae. The ordination space is organized according to the pollen zonation in Fig. 3, with each pollen zone corresponding to compositionally discrete vegetation associations through time. The initial *N. gunnii*–Cupressaceae association

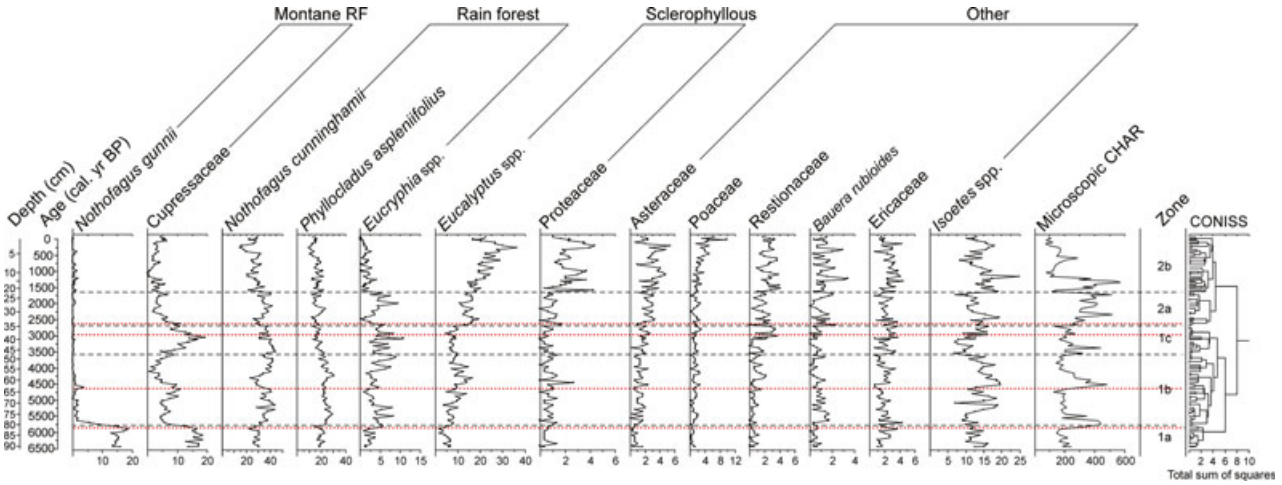

Figure 3 Percentage pollen diagram showing selected taxa from Lake Osborne (core TAS1110SC2). Note the changes in *x*-scale. The *y*-axis is plotted according to age. Pollen zones are delineated by black dashed lines. Red dashed lines indicate the location of the severe fire episodes (*c.* 5856, 4632 and 2966 cal. yr BP; see text for discussion). The unit of measurement for microscopic CHAR (charcoal accumulation rate) is particles cm^{-2} yr^{-1}.

Table 3 Table of principal pollen taxa in the pollen zones identified with the aid of CONISS (Grimm, 1987) for sediment core TAS1110SC2 from Lake Osborne, southern Tasmania. Taxa are listed in order of decreasing importance. Upper and lower age ranges for each zone are also listed.

Pollen zone	Pollen subzone	Lower age (cal. yr BP)	Upper age (cal. yr BP)	Key terrestrial pollen/spores	Key wetland pollen/spores
2	b	−61	1672	*Eucalyptus*, *Nothofagus cunninghamii*, *Phyllocladus aspleniifolius*, Asteraceae, Proteaceae	*Isoetes*
	a	1672	2630	*Nothofagus cunninghamii*, *Eucalyptus*, *Phyllocladus aspleniifolius*, *Eucryphia lucida*	*Isoetes*, *Botryococcus*
1	c	2630	3525	Cupressaceae, *Nothofagus cunninghamii*, *Phyllocladus aspleniifolius*, *Eucalyptus*, *Eucryphia lucida*	*Isoetes*
	b	3525	5786	*Nothofagus cunninghamii*, *Phyllocladus aspleniifolius*, Cupressaceae, *Eucalyptus*, *Eucryphia lucida*	*Isoetes*, *Botryococcus*
	a	5786	6452	*Nothofagus gunnii*, *Cupressaceae*, *Nothofagus cunninghamii*, *Phyllocladus aspleniifolius*	*Isoetes*, *Botryococcus*

(*c.* 6500–5780 cal. yr BP) is the most distinctive of the fossil sequence and was replaced by a *N. cunninghamii–P. aspleniifolius* association between *c.* 5780 and 3530 cal. yr BP. A Cupressaceae–*N. cunninghamii* association prevailed between *c.* 3530 and 2630 cal. yr BP and was replaced by a *N. cunninghamii–Eucalyptus* (*c.* 2630–1670 cal. yr BP) and finally a *Eucalyptus–N. cunninghamii* association (*c.* 1670 cal. yr BP to present).

The cross-correlograms (Fig. 8) display cross-correlation between the 65-cal.-yr interpolated PARs of *Eucryphia*, *N. cunninghamii*, Cupressaceae, *N. gunnii*, N and C with the 65-cal.-yr interpolated macroscopic CHAR data. Significant positive correlations with Cupressaceae and *N. gunnii* occurred for several centuries prior to peak macroscopic CHAR at year zero (Fig. 8). That is, Cupressaceae and *N. gunnii* pollen were most abundant in the centuries prior to increases in macroscopic CHAR, and their values declined rapidly following increases in macroscopic CHAR. Cupressaceae returned to positive correlation after *c.* 1000 cal. yr following increases in macroscopic CHAR, while *N. gunnii* failed to recover following fire. Significant positive correlations of both *Eucryphia* and *N. cunninghamii* with macroscopic CHAR occurred after 520 and 390 cal. yr, respectively, revealing the highest values for these taxa lagging a few centuries after macroscopic CHAR increased. Significant negative correlation with N occurred for over 400 years after peak macroscopic CHAR values (i.e. N values were lowest immediately after macroscopic CHAR peaks).

DISCUSSION

Fire, vegetation and soils

Three severe fire episodes, characterized by large charcoal peaks associated with changes in the pollen spectra and sediment geochemistry, occurred at Lake Osborne between *c.* 6500 and 2900 cal. yr BP, with a return interval of *c.* 1500 yr: *c.* 5856, 4632 and 2966 cal. yr BP (Figs 3–6). Each

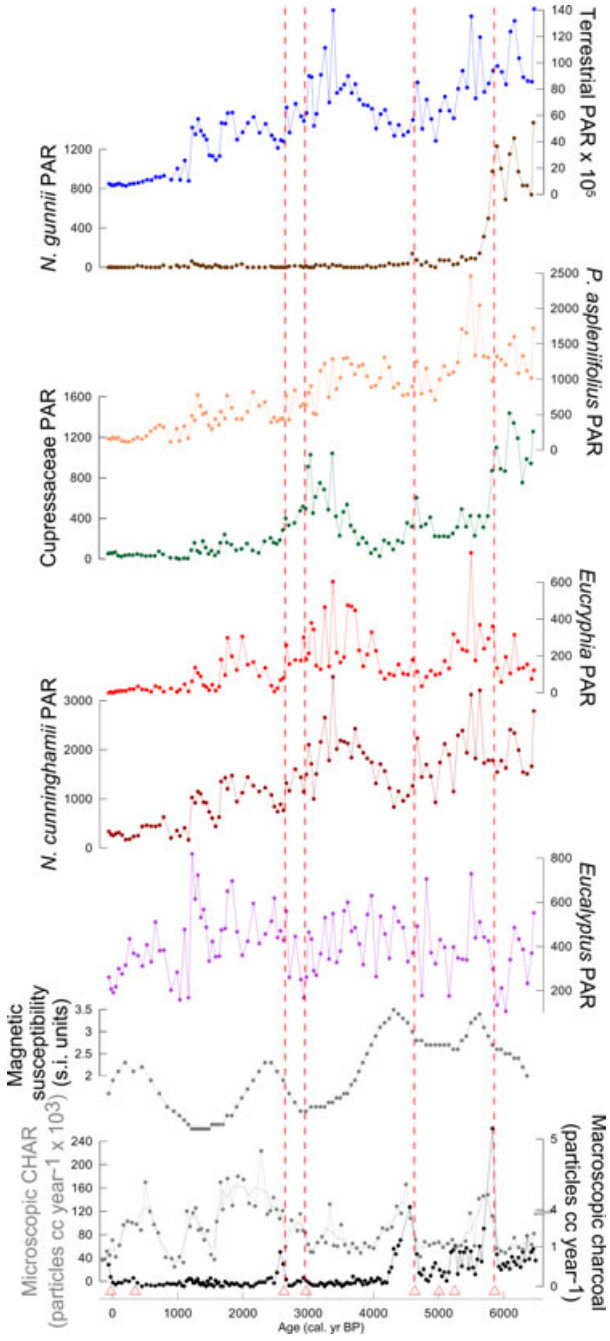

Figure 4 Pollen accumulation rate (PAR) data for all terrestrial plants and selected for taxa from Lake Osborne (core TAS1110SC2). The microscopic CHAR (grey line) and macroscopic CHAR (black line) records and the magnetic susceptibility profile from core TAS1110SC2 are also shown. Red triangles show the location of all statistically significant macroscopic CHAR peaks identified using CharAnalysis (Higuera *et al.*, 2010). Red dashed lines indicate the location of the severe fire episodes (*c.* 5856, 4632 and 2966 cal. yr BP; see text for discussion).

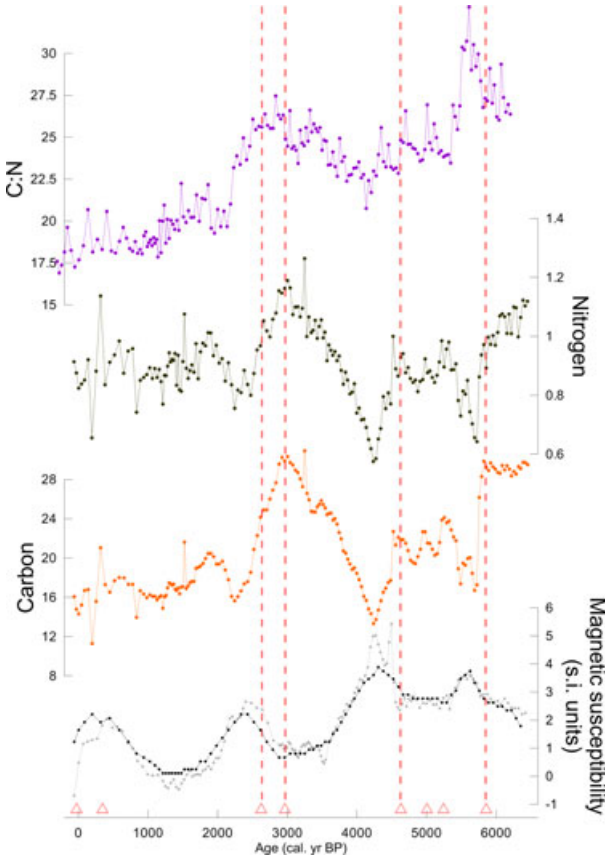

Figure 5 Organic carbon (C) and nitrogen (N) in percentage dry weight, and C:N profiles from Lake Osborne (core TAS1110SC2). Red triangles show the location of all statistically significant macroscopic CHAR peaks identified using CharAnalysis (Higuera *et al.*, 2010). Red dashed lines indicate the location of the severe fire episodes (*c.* 5856, 4632 and 2966 cal. yr BP; see text for discussion).

of these fires was followed by compositionally distinct vegetation associations (Fig. 7). The first fire (5856 cal. yr BP) was associated with the extinction of *N. gunnii*, an endemic montane rain forest tree (Figs 3 & 4), while the widespread rain forest taxa *N. cunninghamii* and *Eucryphia* were able to regenerate within a few centuries of each fire episode (Fig. 8). Importantly, the 800-year post-fire lag of Cupressaceae (probably the montane rain forest tree *Athrotaxis*) reveals a much slower recovery of this conifer than other rain forest tree taxa (Fig. 8). In contrast, *Eucalyptus* displays a much more rapid post-fire response, consistent with the fire ecology of this renowned 'fire-weed' (*sensu* Bowman, 2003). The divergent responses of these arboreal taxa to fire provide critical insights into the long-term dynamics of this vegetation system and the processes in which pyrophytic associations can replace pyrophobic vegetation.

The occurrence of two severe fire episodes within 300 years (*c.* 2900–2600 cal. yr BP) in the Lake Osborne catchment was apparently sufficient to shift pyrophobic coniferous rain forest to pyrophytic *Eucalyptus*-dominated vegetation. This shift was preceded by a suite of changes that paved the way for and subsequently reinforced the persistence of pyrophytic vegetation, including: (1) sequential post-fire changes in the composition of plants surrounding

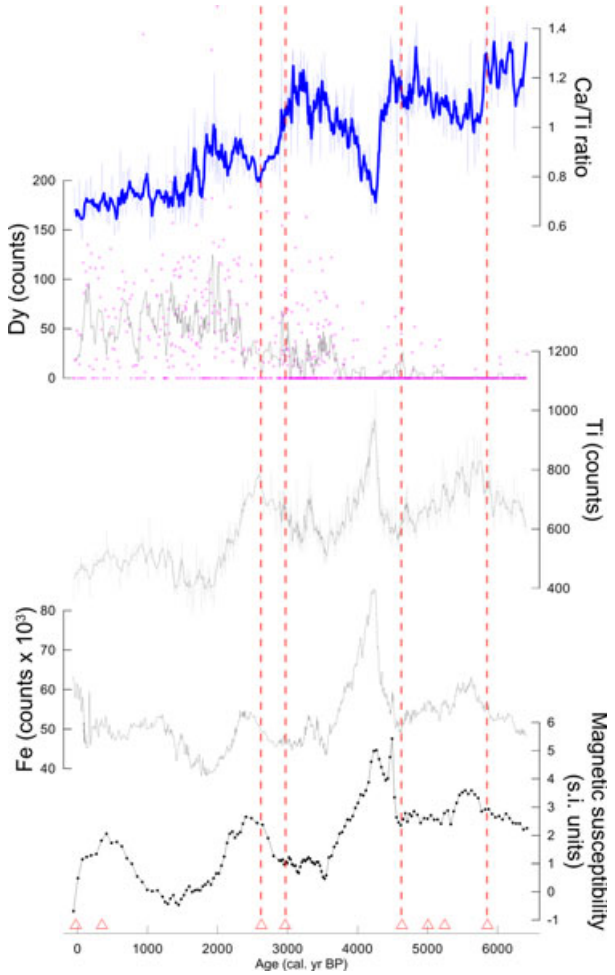

Figure 6 Selected sedimentary elemental data obtained with ITRAX analysis from Lake Osborne (core TAS1110SC1). Red triangles show the location of all statistically significant macroscopic CHAR peaks identified using CharAnalysis (Higuera *et al.*, 2010). Red dashed lines indicate the location of the severe fire episodes (*c.* 5856, 4632 and 2966 cal. yr BP; see text for discussion).

the site, which led to the establishment of pyrogenic *Eucalyptus* species within the catchment (Fig. 7); (2) the loss of soil cover within the catchment after 3800 cal. yr BP, shown by the increase in dysprosium deposition into the lake (the result of weathering of exposed dolerite bedrock within the catchment) (Fig. 6); (3) the loss of important nutrients from the catchment into the lake following successive severe fire episodes (Figs 5 & 6); (4) a transition to a low-biomass open vegetation that is more prone to drying, indicated by the reduction in arboreal PAR and the substantial reduction in organic matter input to the lake (Figs 4, 5 & 9); (5) an increase in sclerophyllous plant taxa (e.g. *Eucalyptus*, *Melaleuca*, *Leptospermum* and Proteaceae) that would have promoted the flammability of the vegetation (Fig. 3 & 10); and (6) a change from a climate-limited fire regime (where discrete charcoal peaks correspond to discrete declines in forest taxa) to a vegetation-limited fire regime (where charcoal changes follow changes in *Eucalyptus* PAR) (Figs 4 & 9).

Interestingly, this state shift from pyrophytic to pyrophobic vegetation was associated with a change in charcoal particle size, with macroscopic charcoal fragments prevailing during the high-biomass rain forest phase and microscopic charcoal deposition being more abundant during the lower-biomass sclerophyllous vegetation phase (Fig. 9). Although shifts in charcoal size fractions are often interpreted as changes in local versus distant source area (Whitlock & Larsen, 2001), we suggest that shifts in fuel biomass may also have influenced the charcoal particle size distribution. A similar conclusion was reached in New Zealand, where macroscopic charcoal abundance declined in association with the initial burning and deforestation that occurred soon after the arrival of Maori (McWethy *et al.*, 2010). Following the loss of New Zealand rain forests, microscopic charcoal particles remained abundant, suggesting the persistent burning of shrub and grassland vegetation.

Recent work on lowland temperate rain forests in south-west Tasmania shows the central role that fire–vegetation–soil feedbacks play in the post-fire dynamics of the lowland temperate vegetation of Tasmania (Wood & Bowman, 2012). Although fire was the direct driver of vegetation change within the higher-elevation Lake Osborne catchment, fire-driven changes in substrate and nutrient dynamics were also clearly important. The oligotrophic substrates of south-west Tasmania foster the development of soils high in organic matter that are susceptible to incineration and subsequent erosion (Pemberton, 1988, 1989). Terrestrially derived organic matter in Lake Osborne decreases and detrital minerals (Fe and Ti) increase for several decades following local severe fire episodes (Figs 5 & 6), indicating a loss of the organic soil profile and the exposure of bedrock to weathering following these fire episodes. A reversal of these trends only occurs after increases in the PAR of key rain forest taxa (*N. cunninghamii* and *Eucryphia*) (Figs 5 & 6), consistent with the importance placed on fire–vegetation–soil feedbacks in lower-elevation systems (Wood & Bowman, 2012). Moreover, non-detrital (biogenic) calcium is high in montane soils that underlie coniferous vegetation in Tasmania (Kirkpatrick, 1997) and is higher in soils formed under cupressaceous vegetation in the Northern Hemisphere than that formed under other conifers and angiosperms (Kiilsgaard *et al.*, 1987). At Lake Osborne, calcium varies in tandem with Cupressaceae PAR (Fig. 9), reflecting an integrated vegetation–soil system response to fire in which severe fire episodes burn the forest and the highly organic soil profile, promoting the loss of nutrients from the catchment. Only after prolonged fire-free intervals does the vegetation recover sufficiently to allow (1) the re-establishment of soil cover within the catchment, and (2) the accumulation of plant-dependent nutrients (such as Ca and N).

Climate variability and fire-driven vegetation change

Inter-annual climate modes, such as the El Niño–Southern Oscillation (ENSO) and the Southern Annular Mode

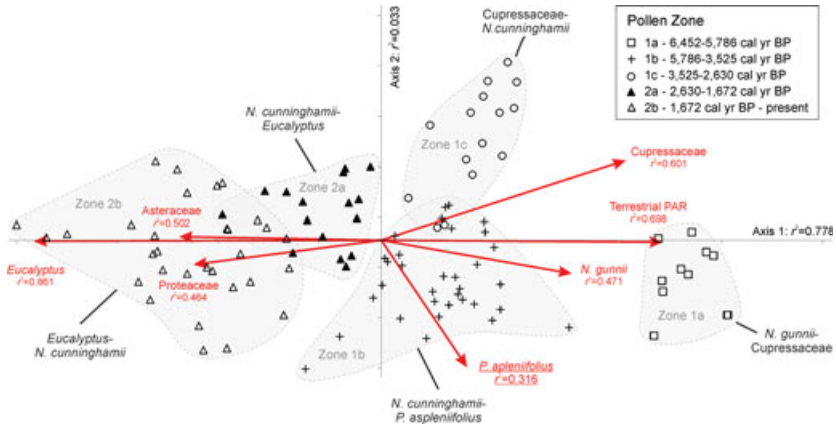

Figure 7 Detrended correspondence analysis (DCA) ordination biplot for the percentage pollen data from Lake Osborne (core TAS1110SC2). Samples are grouped according to pollen zones identified with CONISS (Grimm, 1987); r^2 scores displaying variance in the dataset explained by each ordination axis are shown, as are the direction and strength of correlations between key arboreal taxa and the ordination axes (underscored taxa are correlations with axis 2).

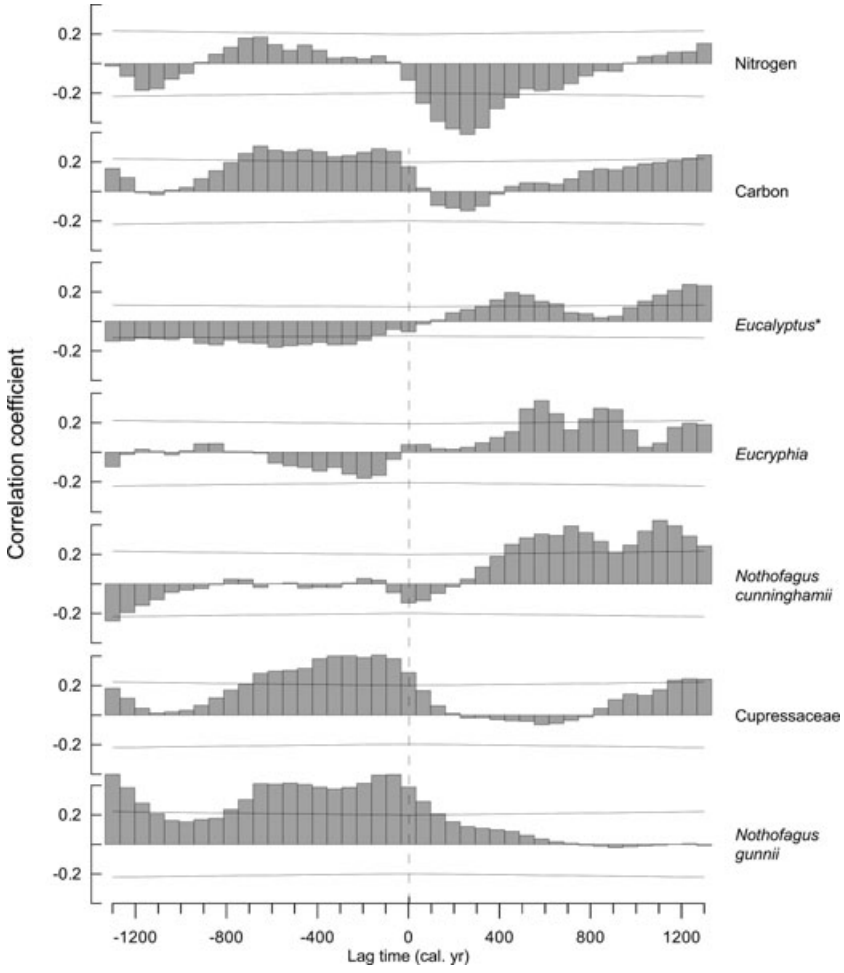

Figure 8 Cross-correlograms obtained through cross-correlation analyses between the 65-year interpolated pollen accumulation rate records of key pollen taxa and C and N stratigraphies and the 65-year interpolated macroscopic CHAR record. The 0.95 confidence limits are indicated as solid lines either side of zero correlation on each graph. * indicates cross-correlation with microscopic CHAR.

(SAM), play a central role in governing decadal-scale to century-scale fire occurrence in south-east Australia and southern South America (Nicholls & Lucas, 2007; Holz & Veblen, 2011; Fletcher & Moreno, 2012a). El Niño events, the warm phase of ENSO, are associated with low rainfall (Hill *et al.*, 2009) and large fires in Tasmania (Nicholls & Lucas, 2007). Consistent with this relationship, the severe fire episodes that occurred at Lake Osborne (*c.* 5856, 4632 and 2966 cal. yr BP) were all associated with periods of very-high-frequency El Niño events in the tropical Pacific Ocean region (Fig. 10), revealing a long-term link between fire in the study region and ENSO. Indeed, changes in the frequency and variability of El Niño events have had wide-ranging impacts on moisture and fire regimes across the Southern Hemisphere (Fletcher & Moreno, 2012b) and, critically, the fire-driven switch from rain forest to *Eucalyptus*-dominated vegetation between 2900–2600 cal. yr BP at Lake Osborne occurred through a marked phase of very strong

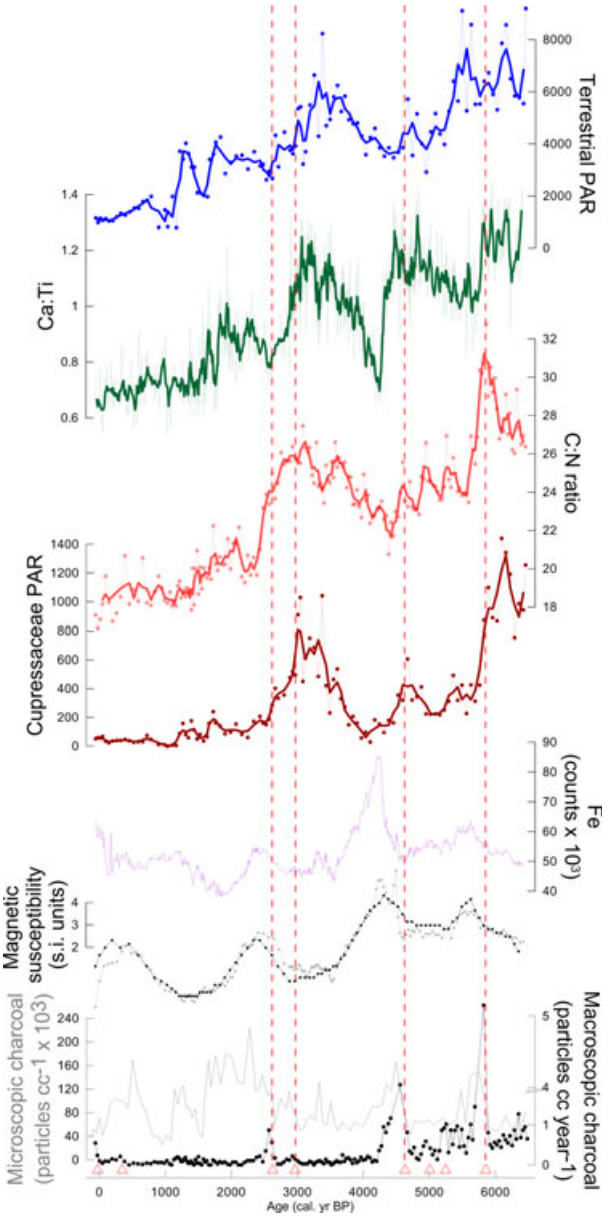

Figure 9 Summary diagram of selected sedimentary profiles from Lake Osborne showing (listed from top to bottom): terrestrial PAR (TAS1110SC2); Ca:Ti ratio (TAS1110SC1); C:N ratio (TAS1110SC2); Cupressaceae PAR (TAS1110SC2); Fe counts (TAS1110SC1); magnetic profiles (grey line, TAS1110SC1; black line, TAS1110SC2); microscopic CHAR (TAS1110SC2, grey line); and macroscopic CHAR (TAS1110SC2; black line). Red triangles show the location of all statistically significant macroscopic CHAR peaks identified using CharAnalysis (Higuera *et al.*, 2010). Red dashed lines indicate the location of the severe fire episodes (*c.* 5856, 4632 and 2966 cal. yr BP; see text for discussion).

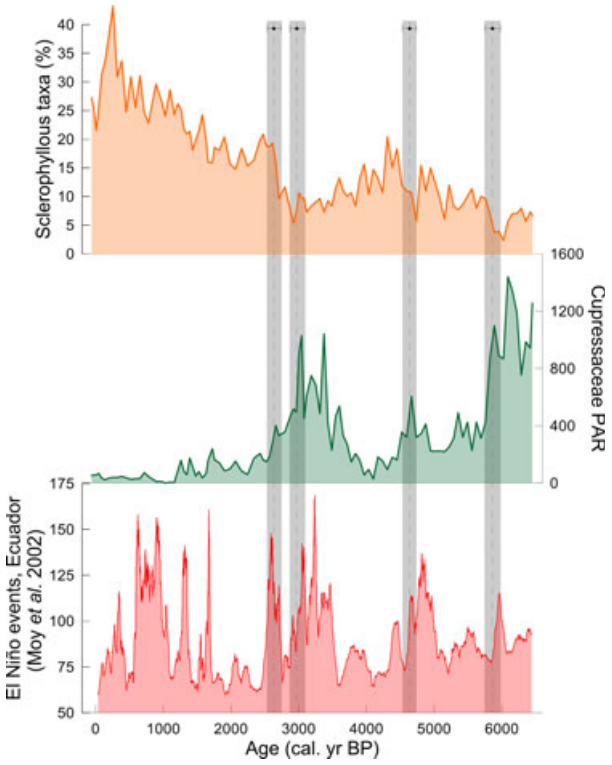

Figure 10 Plot showing the percentage representation of sclerophyllous taxa (*Eucalyptus*, *Leptospermum*, *Melaleuca* and Proteaceae) in the Lake Osborne pollen record, Cupressaceae PAR, and the Laguna Palcacocha El Niño event record from Ecuador (smoothed with a 101-point weighted average filter) (Moy *et al.*, 2002). Vertical dashed lines show the location of statistically significant macroscopic CHAR peaks that were associated with periods of erosion in the Lake Osborne catchment (5856, 4632, 2966 and 2626 cal. yr BP). The grey shaded areas are the 2-sigma error ranges around each macroscopic CHAR peak produced by the age–depth model.

El Niño events that began around 3100 cal. yr BP (Riedinger *et al.*, 2002). Importantly, some climate model projections suggest that the ENSO system is vulnerable to crossing a tipping point due to anthropogenic climate change, with a projected increase in the frequency and intensity of El Niño events in the future (Guilyardi, 2006; Lenton *et al.*, 2008). Thus, our results highlight the sensitivity of endemic montane rain forest in Tasmania to El Niño-driven fires, foreshadowing a further potential stressor for a system that has already suffered widespread fire damage since the arrival of Europeans.

Human amplification of climate-driven fires

Our results provide critical insights into the mechanisms by which mesophytic flora are supplanted by pyrophytic plant taxa. The contraction of Australian mesophytic plant taxa into humid refugia in the east, south-east and far south-west during the late Cenozoic was in response to climatic change wrought by both the northward drift of Australia into the subtropical arid zone and the impact of repeated Quaternary glaciations on the Australian hydroclimate (Hill, 2004; Kershaw *et al.*, 2007). Sniderman & Haberle (2012) highlighted the subordinate role of fire relative to climate in this process, revealing that fire was very rare in the early Pleistocene

coniferous rain forests that occupied part of south-east Australia that now hosts dry *Eucalyptus* forest. Fire frequency at their site increased by an order of magnitude during the climate-driven transitions to sclerophyllous *Eucalyptus*-dominated vegetation that punctuate the early Pleistocene (Sniderman & Haberle, 2012). Our detailed analysis of the Lake Osborne system reveals that fire, although subordinate to the role that climate plays in governing vegetation and fire regimes over long (orbital and tectonic) time-scales, can play a direct role in facilitating the replacement of pyrophobic rain forest by pyrophytic vegetation at smaller spatial and temporal scales. Further, our results reveal that repeated burning can degrade landscapes, retarding post-fire vegetation recovery and favouring the establishment of pyrogenic species that can alter fire regimes in favour of pyrophytic vegetation. This latter process is reminiscent of the impact that the arrival of the Maori had on the analogous *Nothofagus*–Podocarpaceae cool temperate rain forests of New Zealand (McWethy *et al.*, 2010).

The widespread loss of *Athrotaxis* following European colonization highlights the vulnerability of these systems to fire. This raises the question of how Aborigines used fire in western Tasmania and how these ignitions amplified the background fire activity. Our study suggests that fire was a rare occurrence in the study area. This may be because Aboriginal fire use was extraordinarily skilful and targeted, as argued by Gammage (2011). It may also reflect that Aborigines rarely ventured into the high mountains and that fires in these regions were either the result of extreme climate events during which even the most skilful of burning practices could not prohibit the burning of fire-sensitive vegetation, and/or that these fires were caused by lightning. More research is required to chart how fire regimes changed following both Aboriginal and European colonization of Tasmania, coupling studies such as this with archaeological and historical data. What is certain is that Aboriginal fire usage did not limit the re-expansion of forests in many settings at the end of the Pleistocene (Fletcher & Thomas, 2010a,b) – a notion supported by the widespread Late Glacial abandonment of numerous now-forested cave areas in western Tasmania (Cosgrove, 1999), which was probably caused by the return of forests and the displacement of people to an open-site existence where they developed and enhanced alternative economic strategies (Thomas, 1993; Fletcher & Thomas, 2007).

The complexity of the interactions between fire, vegetation and soils, and between natural and culturally distinct fire regimes, signals that extreme care is required when promoting simplistic explanations about the dynamics of pyrophobic and pyrogenic vegetation in the Southern Hemisphere. Resolving the relative roles of each of these key factors that influence fire-driven vegetation dynamics demands comparative studies from around the Southern Hemisphere that illuminate how fire regimes vary across climatic gradients before and after prehistoric and historic human colonization (McWethy *et al.*, 2013).

ACKNOWLEDGEMENTS

M.-S.F. was funded by ARC DIRD Project DI110100019 and Fondecyt 3110180. We also acknowledge support from the US National Science Foundation (OISE 0966472) to C.W. The field programme was supported by ARC DP110101950. Charcoal counting was performed by Rita Attwood at the University of Melbourne. Thanks go to Scott Nichols for help in the field. We thank Peter Kershaw and Vera Markgraf for comments on an earlier draft and Peter Linder for constructive advice.

REFERENCES

Appleby, P.G. & Oldfield, F. (1978) The calculation of lead-210 dates assuming a constant rate of supply unsupported ^{210}Pb to the sediment. *Catena*, **5**, 1–8.

Bennett, K.D. (2005) *Documentation for psimpoll 4.25 and pscomb 1.03: C programs for plotting pollen diagrams and analysing pollen data*. Uppsala University, Uppsala, Sweden.

Binford, M.W. (1990) Calculation and uncertainty analysis of ^{210}Pb dates for PIRLA project lake sediment cores. *Journal of Paleolimnology*, **3**, 253–267.

Blaauw, M. (2010) Methods and code for 'classical' age-modelling of radiocarbon sequences. *Quaternary Geochronology*, **5**, 512–518.

Bond, W.J., Woodward, F.I. & Midgley, G.F. (2005) The global distribution of ecosystems in a world without fire. *New Phytologist*, **165**, 525–537.

Bowman, D.M.J.S. (2000) *Australian rainforests: islands of green in a land of fire*. Cambridge University Press, Cambridge, UK.

Bowman, D.M.J.S. (2003) Australian landscape burning: a continental and evolutionary perspective. *Fire in ecosystems of south-west Western Australia: impacts and management* (ed. by I. Abbott and N. Burrows), pp. 107–118. Backhuys Publishers, Leiden, The Netherlands.

Bowman, D.M.J.S. & Jackson, W. (1981) Vegetation succession in Southwest Tasmania. *Search*, **12**, 358–362.

Bowman, D.M.J.S. & Wood, S.W. (2009) Fire-driven land cover change in Australia and W.D. Jackson's theory of the fire ecology of southwest Tasmania. *Tropical fire ecology: climate change, land use, and ecosystem dynamics* (ed. by M.A. Cochrane), pp. 87–111. Springer, Heidelberg.

Bowman, D.M.J.S., Maclean, A.R. & Crowden, R.K. (1986) Vegetation–soil relations in the lowlands of south-west Tasmania. *Australian Journal of Ecology*, **11**, 141–153.

Bowman, D.M.J.S., Balch, J.K., Artaxo, P. *et al.* (2009) Fire in the Earth system. *Science*, **324**, 481–484.

Cosgrove, R. (1999) Forty-two degrees south: the archaeology of late Pleistocene Tasmania. *Journal of World Prehistory*, **13**, 357–402.

Crisp, M.D., Burrows, G.E., Cook, L.G., Thornhill, A.H. & Bowman, D.M.J.S. (2011) Flammable biomes dominated by eucalypts originated at the Cretaceous–Palaeogene boundary. *Nature Communications*, **2**, 193.

Duncan, D.M. (2003) *Exploration Licence 38/1997 Aberfoyle Hill N.E. Tasmania*. Mineral Holdings Australia, Toorak, Victoria.

Faegri, K. & Iversen, J. (1989) *Textbook of pollen analysis*. Wiley, New York.

Fletcher, M.-S. & Moreno, P.I. (2012a) Vegetation, climate and fire regime changes in the Andean region of southern Chile (38° S) covaried with centennial-scale climate anomalies in the tropical Pacific over the last 1500 years. *Quaternary Science Reviews*, **46**, 46–56.

Fletcher, M.-S. & Moreno, P.I. (2012b) Have the Southern Westerlies changed in a zonally symmetric manner over the last 14,000 years? A hemisphere-wide take on a controversial problem. *Quaternary International*, **253**, 32–46.

Fletcher, M.-S. & Thomas, I. (2007) Holocene vegetation and climate change from near Lake Pedder, south-west Tasmania, Australia. *Journal of Biogeography*, **34**, 665–677.

Fletcher, M.-S. & Thomas, I. (2010a) The origin and temporal development of an ancient cultural landscape. *Journal of Biogeography*, **37**, 2183–2196.

Fletcher, M.-S. & Thomas, I. (2010b) A Holocene record of sea level, vegetation, people and fire from western Tasmania, Australia. *The Holocene*, **20**, 351–361.

Gammage, B. (2011) *The biggest estate on Earth*. Allen and Unwin, Melbourne.

Green, D.G. (1981) Time series and postglacial forest ecology. *Quaternary Research*, **15**, 265–277.

Grimm, E.C. (1987) CONISS: a FORTRAN 77 program for stratigraphically constrained cluster analysis by the method of incremental sum of squares. *Computers and Geosciences*, **13**, 13–35.

Guilyardi, E. (2006) El Niño–mean state–seasonal cycle interactions in a multi-model ensemble. *Climate Dynamics*, **26**, 329–348.

Harris, S. & Kitchener, A. (eds) (2005) *From forest to fjaeldmark: descriptions of Tasmania's vegetation*. Department of Primary Industries, Water and Environment, Hobart.

Head, L. (1985) Further discussion of *Phyllocladus* and its pollen in Victoria during the Holocene. *Australian Journal of Ecology*, **10**, 73–76.

Higuera, P.E., Brubaker, L.B., Anderson, P.M., Hu, F.S. & Brown, T.A. (2009) Vegetation mediated the impacts of postglacial climate change on fire regimes in the south-central Brooks Range, Alaska. *Ecological Monographs*, **79**, 201–219.

Higuera, P.E., Gavin, D.G., Bartlein, P.J. & Hallett, D.J. (2010) Peak detection in sediment–charcoal records: impacts of alternative data analysis methods on fire-history interpretations. *International Journal of Wildland Fire*, **19**, 996–1014.

Hill, R.S. (2004) Origins of the southeastern Australian vegetation. *Philosophical Transactions of the Royal Society B: Biological Sciences*, **359**, 1537–1549.

Hill, R.S. & Carpenter, R.J. (1990) Extensive past distributions for major Gondwanic flora elements: macrofossil evidence. *Papers and Proceedings of the Royal Society of Tasmania*, **124**, 239–247.

Hill, M.O. & Gauch, H.G., Jr (1980) Detrended correspondence analysis: an improved ordination technique. *Vegetatio*, **42**, 47–58.

Hill, K.J., Santoso, A. & England, M.H. (2009) Interannual Tasmanian rainfall variability associated with large-scale climate modes. *Journal of Climate*, **22**, 4383–4397.

Holz, A. & Veblen, T.T. (2011) Variability in the Southern Annular Mode determines wildfire activity in Patagonia. *Geophysical Research Letters*, **38**, L14710.

Jackson, W.D. (1968) Fire, air, water and earth – an elemental ecology of Tasmania. *Proceedings of the Ecological Society of Australia*, **3**, 9–16.

Jackson, W.D. (1999) The Tasmanian environment. *Vegetation of Tasmania* (ed. by J.B. Reid, R.S. Hill, M.J. Brown and M.J. Hovenden), pp. 11–38. Australian Biological Resources Study, Canberra.

Kershaw, A.P., McKenzie, G.M., Porch, N., Roberts, R.G., Brown, J., Heijnis, H., Orr, M.L., Jacobsen, G. & Newall, P.R. (2007) A high-resolution record of vegetation and climate through the last glacial cycle from Caledonia Fen, southeastern highlands of Australia. *Journal of Quaternary Science*, **22**, 481–500.

Kiilsgaard, C.W., Greene, S.E. & Stafford, S.G. (1987) Nutrient concentrations in litterfall from some western conifers with special reference to calcium. *Plant and Soil*, **102**, 223–227.

Kirkpatrick, J.B. (1997) *Alpine Tasmania: an illustrated guide to the flora and vegetation*. Oxford University Press, Melbourne.

Kirkpatrick, J.B. & Dickinson, K.J.M. (1984) The impact of fire on Tasmanian alpine vegetation and soils. *Australian Journal of Botany*, **32**, 613–629.

Lenton, T.M., Held, H., Kriegler, E., Hall, J.W., Lucht, W., Rahmstorf, S. & Schellnhuber, H.J. (2008) Tipping elements in the Earth's climate system. *Proceedings of the National Academy of Sciences USA*, **105**, 1786–1793.

McCormac, F.G., Hogg, A.G., Blackwell, P.G., Buck, C.E., Higham, T.F.G. & Reimer, P.J. (2004) SHCal04 Southern Hemisphere calibration, 0–11.0 cal kyr BP. *Radiocarbon*, **46**, 1087–1092.

McCune, B. & Mefford, M.J. (1999) *PC-Ord for Windows*. MjM Software, Gleneden Beach, OR.

McKenzie, G.M. & Kershaw, A.P. (2000) The last glacial cycle from Wyelangta, the Otway region of Victoria, Australia. *Palaeogeography, Palaeoclimatology, Palaeoecology*, **155**, 177–193.

McWethy, D.B., Whitlock, C., Wilmshurst, J.M., McGlone, M.S., Fromont, M., Li, X., Dieffenbacher-Krall, A., Hobbs, W.O., Fritz, S.C. & Cook, E.R. (2010) Rapid landscape transformation in South Island, New Zealand, following initial Polynesian settlement. *Proceedings of the National Academy of Sciences USA*, **107**, 21343–21348.

McWethy, D.B., Higuera, P.E., Whitlock, C., Veblen, T.T., Bowman, D.M.J.S., Cary, G.J., Haberle, S.G., Keane, R.E., Maxwell, B.D., McGlone, M.S., Perry, G.L.W., Wilmshurst, J.M., Holz, A. & Tepley, A.J. (2013) A conceptual framework for predicting temperate ecosystem sensitivity to

human impacts on fire regimes. *Global Ecology and Biogeography*, **22**, 900–912.

Meyers, P.A. & Teranes, J.L. (2001) Sediment organic matter. *Tracking environmental change using lake sediments.* Vol. 2. *Physical and geochemical methods* (ed. by W.M. Last and J.P. Smol), pp. 239–269. Kluwer Academic Publishers, Dordrecht, The Netherlands.

Moy, C.M., Seltzer, G.O., Rodbell, D.T. & Anderson, D.M. (2002) Variability of El Niño/Southern Oscillation activity at millennial timescales during the Holocene epoch. *Nature*, **420**, 162–165.

Nicholls, N. & Lucas, C. (2007) Interannual variations of area burnt in Tasmanian bushfires: relationships with climate and predictability. *International Journal of Wildland Fire*, **16**, 540–546.

Pemberton, M. (1988) Soil erosion between Birchs Inlet and Elliott Bay, southwestern Tasmania. *Papers and Proceedings of the Royal Society of Tasmania*, **122**, 109–114.

Pemberton, M. (1989) *Land systems of Tasmania (south west)*. Tasmanian Government Printer, Hobart.

R Core Development Team (2008) *R: a language and environment for statistical computing*. R Foundation for Statistical Computing, Vienna, Austria.

Riedinger, M.A., Steinitz-Kannan, M., Last, W.M. & Brenner, M. (2002) A ~6100 ^{14}C yr record of El Niño activity from the Galápagos Islands. *Journal of Paleolimnology*, **27**, 1–7.

Sniderman, J.M.K. & Haberle, S.G. (2012) Fire and vegetation change during the Early Pleistocene in southeastern Australia. *Journal of Quaternary Science*, **27**, 307–317.

Sturman, A.P. & Tapper, N.J. (2006) *The weather and climate of Australia and New Zealand*. Oxford University Press, New York.

Thomas, I. (1993) Late Pleistocene environments and Aboriginal settlement patterns in Tasmania. *Australian Archaeology*, **36**, 1–11.

Thomas, I., Cullen, P. & Fletcher, M.-S. (eds) (2010) *Ecological drift or stable fire cycles in Tasmania: a resolution?* Australian National University Press, Canberra.

Whitlock, C. & Larsen, C. (2001) Charcoal as a fire proxy. *Tracking environmental change using lake sediments.* Vol. 3. *Terrestrial, algal, and siliceous indicators* (ed. by J.P. Smol, H.J.B. Birks and W. M. Last), pp. 75–97. Kluwer Academic Publishers, Dordrecht, The Netherlands.

Wood, S.W. & Bowman, D.M.J.S. (2012) Alternative stable states and the role of fire–vegetation–soil feedbacks in the temperate wilderness of southwest Tasmania. *Landscape Ecology*, **27**, 1–16.

Wood, S.W., Hua, Q., Allen, K.J. & Bowman, D.M.J.S. (2010) Age and growth of a fire prone Tasmanian temperate old-growth forest stand dominated by *Eucalyptus regnans*, the world's tallest angiosperm. *Forest Ecology and Management*, **260**, 438–447.

Wood, S.W., Murphy, B.P. & Bowman, D.M.J.S. (2011) Firescape ecology: how topography determines the contrasting distribution of fire and rain forest in the southwest of the Tasmanian Wilderness World Heritage Area. *Journal of Biogeography*, **38**, 1807–1820.

SUPPORTING INFORMATION

Additional Supporting Information may be found in the online version of this article:

Appendix S1 Lake Osborne magnetic susceptibility and macroscopic charcoal analyses.

Appendix S2 Lake Osborne macroscopic charcoal analysis.

BIOSKETCH

Michael-Shawn Fletcher is interested in the long-term interactions between humans, climate, disturbance and vegetation at local, regional and global scales. This project is aligned with the WildFIRE PIRE collaborative (http://www.wildfirepire.org/).

Author contributions: M.-S.F. conceived the paper; M.-S.F conducted the pollen, spore and charcoal analyses; M.-S.F. and B.B.W. conducted the elemental analyses; M.-S.F., H.H. and P.S.G. conducted the ITRAX analysis; D.P.P. conducted the ^{210}Pb analyses; M.-S.F led the writing; and B.B.W., C.W., D.P.P., H.H., S.G.H., P.S.G. and D.M.J.S.B. contributed to the writing.

Editor: Peter Linder